DETERMINATION OF DEPENDENCE OF GRAVITATIONAL INTERACTION FORCE OF BODIES ON THEIR VELOCITY

© 2021 **A. A. Gribkov***

Moscow State Technological University "STANKIN", Moscow

This article presents the results of testing the hypothesis of the dependence of gravity on the velocity of motion of bodies. The numerical simulation clearly confirmed the correspondence of the calculated and observed values of the precession of orbit pericentres in binary systems including pulsars, as well as planets of the solar system. Based on the revealed dependence of the gravitational force on the velocity, the article describes a new effect of the precession of the centres of binary systems, which should be found as a result of further practical research.

Keywords: gravity, binary systems, pulsars

I. INTRODUCTION

The assumption that the force of gravitational interaction of bodies depends on the velocity of their motion is not new. The theories of Ritz, Gerber, and others suggested such an influence. Einstein's special theory of relativity also assumes the influence of the motion velocity of bodies on their gravity force (through changes in mass). In this paper, we propose to test the hypothesis that the force of gravitational attraction depends on the velocities of interacting bodies as follows:

$$\begin{aligned} F_{1\leftarrow 2} &= \frac{GM_1M_2}{r^2}\left(1+\frac{v_2^2}{w^2}\right)^{\mu/2}\left(1+\frac{v_1^2}{w^2}\right)^{\lambda/2} \approx \frac{GM_1M_2}{r^2}\left(1+\frac{\mu v_2^2+\lambda v_1^2}{2w^2}\right), \\ F_{2\leftarrow 1} &= \frac{GM_1M_2}{r^2}\left(1+\frac{v_1^2}{w^2}\right)^{\mu/2}\left(1+\frac{v_2^2}{w^2}\right)^{\lambda/2} \approx \frac{GM_1M_2}{r^2}\left(1+\frac{\mu v_1^2+\lambda v_2^2}{2w^2}\right), \end{aligned} \tag{1}$$

where $F_{1\leftarrow 2}$, $F_{2\leftarrow 1}$ are the forces acting, respectively, from the 2-th body (with mass M_2) on the 1st (with mass M_1) and from the 1st body on 2nd, v_1, v_2 — absolute velocity of the 1st and 2nd bodies, r — current distance between the bodies, μ — exponent with which the

*E-mail: andarmo@yandex.ru

velocity of the gravitation source defines the force of gravity, λ — exponent with which the velocity of the "recipient" of gravity (the object on which gravity acts) defines the gravity force, w — a constant having the dimension of velocity ($w \gg v_1$, $w \gg v_2$).

A key indicator of compliance with the proposed hypotheses regarding the gravity of reality the last hundred years is the ability to use them to explain the precession of pericentres of binary systems components (initially it was about the precession of the perihelion of Mercury and the other planets of the solar system). This effect mainly manifests in binary neutron stars (at least one of the neutron stars is a pulsar), binary systems of a neutron star (pulsar) and a white dwarf, and under certain conditions — in binary systems of a neutron star (pulsar) and a main-sequence star. Besides, the study of this effect in the solar system is of considerable interest.

II. NUMERICAL SIMULATION OF ORBITAL MOTION

A. Numerical simulation algorithm

For different variants of the dependence of the gravity force on velocity (i.e. different μ, λ and w), numerical step-by-step simulation of the motion of the components of the binary system was performed in this work. Let us briefly outline the sequence of calculations.

Time interval corresponding to each step:

$$\tau = \frac{P_b}{N}, \tag{2}$$

where P_b is the orbital period of the binary system, N is the number of steps per period.

Let's determine the acting forces of gravity:

$$\begin{aligned} \left|F_{1\leftarrow 2|i}\right| &= \frac{k}{r_{i-1}^2}\left(1+\frac{v_{2|i-1}^2}{w^2}\right)^{\mu/2}\left(1+\frac{v_{1|i-1}^2}{w^2}\right)^{\lambda/2}, \\ \left|F_{2\leftarrow 1|i}\right| &= \frac{k}{r_{i-1}^2}\left(1+\frac{v_{1|i-1}^2}{w^2}\right)^{\mu/2}\left(1+\frac{v_{2|i-1}^2}{w^2}\right)^{\lambda/2}, \end{aligned} \tag{3}$$

where $k = GM_1M_2$ is a constant coefficient determined by the gravitational constant G and the masses of the components M_1 and M_2; $r_{i-1} = \sqrt{\left(x_{1|i-1} - x_{2|i-1}\right)^2 + \left(y_{1|i-1} - y_{2|i-1}\right)^2}$ — the distance between the interacting components at the previous step, $x_{1|i-1}, x_{2|i-1}, y_{1|i-1}, y_{2|i-1}$ — the coordinates of the components at the previous step.

Decompose the forces along the axes:

$$\begin{aligned} F_{1\leftarrow 2|iX} &= \frac{x_{2|i-1} - x_{1|i-1}}{r_{i-1}} \left|F_{1\leftarrow 2|i}\right|; F_{1\leftarrow 2|iY} = \frac{y_{2|i-1} - y_{1|i-1}}{r_{i-1}} \left|F_{1\leftarrow 2|i}\right|; \\ F_{2\leftarrow 1|iX} &= \frac{x_{2|i-1} - x_{1|i-1}}{r_{i-1}} \left|F_{2\leftarrow 1|i}\right|; F_{1\leftarrow 2|iY} = \frac{y_{2|i-1} - y_{1|i-1}}{r_{i-1}} \left|F_{2\leftarrow 1|i}\right|; \end{aligned} \tag{4}$$

Determine the velocity of the components:

$$\begin{aligned} v_{1|iX} &= v_{1|(i-1)X} + \tau \cdot \frac{F_{1\leftarrow 2|iX}}{M_1}; \; v_{1|iY} = v_{1|(i-1)Y} + \tau \cdot \frac{F_{1\leftarrow 2|iY}}{M_1}; \\ v_{2|iX} &= v_{2|(i-1)X} + \tau \cdot \frac{F_{2\leftarrow 1|iX}}{M_2}; \; v_{2|iY} = v_{2|(i-1)Y} + \tau \cdot \frac{F_{2\leftarrow 1|iY}}{M_2}; \\ v_{1|i} &= \sqrt{v_{1|iX}^2 + v_{1|iY}^2}; \; v_{2|i} = \sqrt{v_{2|iX}^2 + v_{2|iY}^2}. \end{aligned} \tag{5}$$

Component coordinates:

$$\begin{aligned} x_{1|i} &= x_{1|i-1} + \frac{\tau}{2} \cdot \left(v_{1|(i-1)X} + v_{1|iX}\right); \; y_{1|i} = y_{1|i-1} + \frac{\tau}{2} \cdot \left(v_{1|(i-1)Y} + v_{1|iY}\right); \\ x_{2|i} &= x_{2|i-1} + \frac{\tau}{2} \cdot \left(v_{2|(i-1)X} + v_{2|iX}\right); \; y_{2|i} = y_{2|i-1} + \frac{\tau}{2} \cdot \left(v_{2|(i-1)Y} + v_{2|iY}\right). \end{aligned} \tag{6}$$

The initial positions and velocities of the components are determined by the available data on the masses of the components, the orbital period, and the eccentricity of the orbit at the time the components are in the apocenters of their orbits.

The simulation was carried out with the number of steps per system period $N = 1.0 \times 10^6$ for $n = 10$ periods. During the simulation, the positions were determined in which the distance between the system components reached the maximum value (the positions of apocenters; they were used instead of the pericentre positions because they correspond to a lower velocity of motion and, accordingly, are more accurately determined). For such positions, refinement was carried out with a minimum step (up to $1/2^{10}$ of the nominal) and the angle φ_j was found between the apses line and x-axis:

$$\varphi_j = \arcsin\left[\left(y_{1(j)} - y_{2(j)}\right)/r_j\right], \tag{7}$$

where is the current value of the maximum distance between the system components; $y_{1(j)}$, $y_{2(j)}$ — coordinate values of y components corresponding to r_j.

The precession value of the pericentre (or apocentre, or apse line) was determined as follows:

$$\dot{\omega} = \frac{180}{\pi} \frac{P_\oplus}{nP_b} \sum_{j=1}^{n} (\varphi_j - \varphi_{j-1}), \; ^\circ/\text{year}, \tag{8}$$

where $P_\oplus = 3.156 \times 10^7$ sec is the duration of the year.

B. Numerical simulation results

Numerical simulation of different variants of the dependence of the gravitational force on the velocity of the source and "recipient" of gravity (binary neutron stars, neutron star + white dwarf systems, neutron star + yellow dwarf (G dwarf star) systems, as well as planets of the solar system) showed that the simulation results correspond to the existing data of real observations at $\mu = 3\kappa$, $\lambda = 1\kappa$ (κ is a constant multiplier):

$$\begin{aligned} F_{1\leftarrow 2} &= \frac{GM_1M_2}{r^2}\left(1+\frac{v_2^2}{w^2}\right)^{3\kappa/2}\left(1+\frac{v_1^2}{w^2}\right)^{\kappa/2} \approx \frac{GM_1M_2}{r^2}\left(1+\kappa\frac{3v_2^2+v_1^2}{2w^2}\right), \\ F_{2\leftarrow 1} &= \frac{GM_1M_2}{r^2}\left(1+\frac{v_1^2}{w^2}\right)^{3\kappa/2}\left(1+\frac{v_2^2}{w^2}\right)^{\kappa/2} \approx \frac{GM_1M_2}{r^2}\left(1+\kappa\frac{3v_1^2+v_2^2}{2w^2}\right). \end{aligned} \tag{9}$$

For $\kappa = 1$, the value $w = 1.2247 \times 10^8$ m/s ($= c/\sqrt{6}$, where c is the velocity of light). The results of numerical simulation of the motion of components of binary neutron stars are given below, see tables I-II. As can be seen, the calculated data correspond with fairly high accuracy to the observed (or currently assumed) data.

Along with binary neutron stars, systems of a neutron star and a white dwarf can be used as an object for studying subtle gravitational effects. As a result of consideration of four such systems (for which the most complete and reliable data are available), confirmation of the presence of the assumed dependence of gravity on the velocity of motion was obtained (see table III).

In the course of the research, the motions of the binary system components from the J1903+0327 pulsar and the dwarf star (a G-type main-sequence star with a mass of the order of the mass of the Sun) were simulated. Yellow dwarfs are relatively stable stars, which are not characterized by many effects that can affect the displacement of the apse line (for example, the intense mass loss characteristic of large stars, especially in binary systems). The simulation confirmed the validity of the assumption about the dependence of gravity on the motion velocity.

An important role in confirming the considered dependence of gravity on the velocities of the source and the "recipient" plays the analysis of the perihelion precession of the orbits of solar system planets: Mercury, Venus, Earth and Mars (data on other planets are extremely inaccurate), as well as asteroids (data are available only for Icarus). The importance of analyzing the planet orbits is due to the huge difference in the masses of the considered

TABLE I. Precession of the pericentres of binary neutron stars

Parameter		Binary neutron stars (BNS)					
PSR		B1913+16	J0737-3039	B1534+12	B2127+11C	J1518+4904	J1811-1736
Initial data							
Data source		[1]	[2]	[3]	[4]	[5]	[6]-[8]
Orbital period, P_b, s		27907	8835	36352	28968	7.46×10^5	1.63×10^6
Orbital eccentricity, e		0.617	0.088	0.274	0.681	0.249	0.828
Periastron advance, $\dot{\omega}$, °/year		4.227	16.88(10)	1.756	4.464	0.01137	0.009(2)
Masses, $M_\odot$	M_1	1.441	1.337(1)	1.333(1)	1.358(10)	$1.05^{+1.21}_{-0.14}$	1.17 . . . 1.6
	M_2	1.387	1.250(1)	1.345(1)	1.354(10)	$1.56^{+0.20}_{-1.20}$	0.93 . . . 1.5
Selection of the most probable mass values							
Masses, $M_\odot$	M_1	1.441	1.337	1.333	1.358	1.05	1.35**
	M_2	1.387	1.250	1.345	1.354	1.67*	1.22***
Simulation results for $\mu = 3$, $\lambda = 1$, $w = 1.2247 \times 10^8$ m/s							
$\dot{\omega}$, °/year		4.225(4)[σ]	16.878(7)[σ]	1.754(1)[σ]	4.461(5)[σ]	0.01134(12)[σ]	0.00901(5)[σ]

* — total mass of the system $M_1 + M_2 = 2.7183(7)M_\odot$

** — average observed mass of the pulsar

*** — based on the total mass of the system $M_1 + M_2 = 2.57(10)M_\odot$

cosmic bodies and the Sun, which makes the interaction "one-sided": the Sun acts on these bodies, and their influence on the Sun is negligible (Jupiter and Saturn are not included in the number of planets under consideration). The numerical simulation results are consistent with the observational results (see table IV).

C. Determining the empirical relationship

For determining the empirical formula (reproduced by the proposed mathematical model) of the dependence of the calculated value of pericentre precession on the input parameters (the mass of the components M_1 and M_2, the orbital period of the system P_b, the eccentricity of the orbits e, the constant w, the gravitational constant G) at $\mu = 3$, $\lambda = 1$, the parameter values were varied (separately M_1, M_2, P_b, e, w and G with constant other parameters). By varying M_1 and M_2, we studied the change in precession depending on the function $f_2 = e^\xi \times (1 - e^2)^\zeta$ (α, β, ξ, ζ are constants). As a result, we have the following empirical

TABLE II. Precession of the pericentres of binary neutron stars (continued)

Parameter		Binary neutron stars (BNS)				
PSR		J0453+1559	J1756-2251	J1906+0746*	J1829+2456	J1930-1852
Initial data						
Data source		[9]	[10]	[11]	[12], [13]	[14]
Orbital period, P_b, s		3.519×10^5	2.762×10^4	1.434×10^4	1.016×10^5	3.893×10^6
Orbital eccentricity, e		0.1125	0.1806	0.085	0.1391	0.3989
Periastron advance, $\dot{\omega}$, °/year		0.0379	2.582	7.584	0.2919(16)	0.00078(4)
Masses, $M_\odot$	M_1	1.559 ± 0.005	1.341(7)	1.291 ± 0.011	< 1.38**	< 1.32***
	M_2	1.174 ± 0.004	1.230(7)	1.322 ± 0.011	> 1.22**	> 1.3***
Selection of the most probable mass values						
Masses, $M_\odot$	M_1	1.559	1.341	1.291	1.3 ± 0.08	1.2 ± 0.1
	M_2	1.174	1.230	1.322	1.3 ∓ 0.08	1.4 ∓ 0.1
Simulation results for $\mu = 3$, $\lambda = 1$, $w = 1.2247 \times 10^8$ m/s						
$\dot{\omega}$, °/year		0.0379(4)[σ]	2.580(9)[σ]	7.576(12)[σ]	0.2926(11)[σ]	0.000782(15)[σ]

* — there are doubts that the companion of the pulsar is a neutron star, and not a white dwarf [11]

** — total mass of the system $M_1 + M_2 = 2.5(2)M_\odot$

*** — total mass of the system $M_1 + M_2 = 2.59(4)M_\odot$

formula for calculating the pericentre precession value:

$$\dot{\omega}_e = 10.7(1) \times \frac{G^{2/3}(M_1 + M_2)^{2/3}}{w^2 P_b^{5/3}\,(1 - e^2)}. \tag{10}$$

Taking into account that $(2\pi)^{5/3}\Big/2 = 10.697$, $w = c\big/\sqrt{6}$ we get:

$$\dot{\omega}_e \approx \frac{3\,G^{2/3}(M_1 + M_2)^{2/3}}{c^2\left(\frac{P_b}{2\pi}\right)^{5/3}(1 - e^2)}. \tag{11}$$

The right part of the formula (11) completely coincides with the formula for the precession of the pericentre in general relativit [4] and (in the case of $M_1 \gg M_2$ or $M_1 \ll M_2$) — in Gerber's theory [24].

III. PRECESSION OF BINARY SYSTEMS BARYCENTERS

The force acting from the 1st component on the 2nd is not equal to the force acting from the 2nd component on the 1st. As a result, a force F_c acts on the system barycenter.

TABLE III. Precession of the pericentres of the binary systems [neutron star + white dwarf] (NS+WD) and the system [neutron star + G-type dwarf star] (NS+GDS)

Parameter		NS+WD				NS+GDS
PSR		J1141-6545	B2303+46	B1802-07	J0621+1002	J1903+0327
Initial data						
Data source		[15] - [17]	[18]	[19]	[20]	[21], [22]
Orbital period, P_b, s		1.708×10^4	1.066×10^6	2.26×10^5	7.19×10^5	8.22×10^6
Orbital eccentricity, e		0.1719	0.658	0.212	0.00246	0.437
Periastron advance, $\dot{\omega}$, °/year		5.3084(9)	0.0099(2)	0.058(2)	0.0116(8)	$2.400(2) \times 10^{-4}$
Masses, $M_\odot$	M_1	1.27(1)	1.16(28)	$1.26^{+0.15}_{-0.67}$	$1.70^{+0.32}_{-0.29}$	1.667(21)
	M_2	1.02(1)	1.37(24)	$0.36^{+0.56}_{-0.22}$	$0.97^{+0.27}_{-0.15}$	1.029(8)
Selection of the most probable mass values						
Masses, $M_\odot$	M_1	1.27	1.16	1.26	1.70	1.667
	M_2	1.02	1.37	0.36	0.97	1.029
Simulation results for $\mu = 3$, $\lambda = 1$, $w = 1.2247 \times 10^8$ m/s						
$\dot{\omega}$, °/year		5.306(10)[σ]	0.00992(2)[σ]	0.0578(3)[σ]	0.010(1)[σ]	$2.40(4) \times 10^{-4}$ [σ]

TABLE IV. Solar system's 'anomalous' perihelion precession of planetary orbits

Parameter		Planets				Asteroid
		Mercury	Venus	Earth	Mars	Icarus
Initial data [23]						
Orbital period, P_b, s		7.6005×10^6	1.9414×10^7	3.1558×10^7	5.9329×10^7	3.5320×10^7
Orbital eccentricity, e		0.2056	0.0068	0.0167	0.0934	0.82684
Perihelion precession, $\dot{\omega}$, ″/century		43.1 ± 0.5	8.4 ± 4.8	5.0 ± 1.2	1.1 ± 0.3	9.8 ± 0.8
Masses, kg	M_p	3.2868×10^{23}	4.8107×10^{24}	5.976×10^{24}	6.3345×10^{23}	2.9×10^{12}
	$M_\odot$	1.989×10^{30}				
Simulation results* for $\mu = 3$, $\lambda = 1$, $w = 1.2247 \times 10^8$ m/s						
$\dot{\omega}$, ″/century		43.01(1)[σ]	8.623(2)[σ]	3.837(1)[σ]	1.3510(1)[σ]	10.13(5)[σ]

* — the simulation used a variation of the value $w = 1.2247 \times 10^6 \ldots 1.2247 \times 10^8$ m/s

For further analysis, it is necessary to determine the reference system and set the direction of motion of the components along their orbits. For the initial one we take a position in which the components are in the apocenters of their orbits, the component with mass M_1 is located to the right of the system barycenter, the component with mass M_2 on the left; the components move counterclockwise along their orbits; the x-axis is directed from left to right, the y-axis from bottom to top; the angle θ between the x-axis and the radius vector of the 1st component is measured from the positive direction of the x-axis.

Let's determine the force F_c:

$$F_c = F_{2\leftarrow 1} - F_{1\leftarrow 2} = \frac{GM_1M_2}{r^2}\frac{\kappa\left(v_1^2 - v_2^2\right)}{w^2}, \tag{12}$$

where $r = a\left(1-e^2\right)\left(1-e\cos\theta\right)^{-1}$ (e is the system eccentricity, a is the semi-major axis of the relative orbit of the system),

$$v_1 = \frac{1}{\sqrt{1-e^2}}\frac{M_2}{M_1+M_2}\sqrt{\frac{G\left(M_1+M_2\right)}{a}}\sqrt{1+e^2-2e\cos\theta},$$
$$v_2 = \frac{1}{\sqrt{1-e^2}}\frac{M_1}{M_1+M_2}\sqrt{\frac{G\left(M_1+M_2\right)}{a}}\sqrt{1+e^2-2e\cos\theta}.$$

After substitution, we get:

$$F_c = \frac{G^2M_1M_2\left(M_1-M_2\right)\kappa}{a^3w^2\left(1-e^2\right)^3}\left(1-e\cos\theta\right)^2\left(1+e^2-2e\cos\theta\right). \tag{13}$$

Let's find the average value of F_c for the P_b period of the system (assuming no precession of the pericentre):

$$\overline{F_c} = \frac{1}{P_b}\int\limits_0^{P_b} F_c\,dt = \frac{1}{P_b}\int\limits_0^{L} F_c\frac{dl}{v}, \tag{14}$$

where L is the perimeter of the relative elliptical orbit, dl is the elementary path along the relative orbit,

$$v = v_1 + v_2 = \frac{1}{\sqrt{1-e^2}}\sqrt{\frac{G\left(M_1+M_2\right)}{a}}\sqrt{1+e^2-2e\cos\theta},$$
$$dl = a\left(1-e^2\right)\frac{\sqrt{1+e^2-2e\cos\theta}}{\left(1-e\cos\theta\right)^2}d\theta;\quad a = \sqrt[3]{\frac{GP_b^2\left(M_1+M_2\right)}{4\pi^2}}.$$
$$\frac{dl}{v} = \frac{P_b}{2\pi}\frac{\left(1-e^2\right)^{3/2}}{\left(1-e\cos\theta\right)^2}d\theta.$$

Average (time-based) value of the projection of the force F_c on the x-axis (assuming no precession of the pericentre):

$$\begin{aligned}\overline{F_{cX}} &= \frac{2\pi\kappa}{(1-e^2)^{3/2}}\frac{GM_1M_2}{P_b^2w^2}\frac{M_1-M_2}{M_1+M_2}\int\limits_0^{2\pi}\cos\theta\left(1+e^2-2e\cos\theta\right)d\theta = \\ &= \frac{4\pi^2\kappa e}{(1-e^2)^{3/2}}\frac{GM_1M_2}{P_b^2w^2}\frac{M_2-M_1}{M_1+M_2}.\end{aligned} \tag{15}$$

Average (time-based) value of the projection of the force F_c on the y-axis (assuming no precession of the pericentre):

$$\overline{F_{cY}} = \frac{2\pi\kappa}{(1-e^2)^{3/2}}\frac{GM_1M_2}{P_b^2w^2}\frac{M_1-M_2}{M_1+M_2}\int\limits_0^{2\pi}\sin\theta\left(1+e^2-2e\cos\theta\right)d\theta = 0. \tag{16}$$

As a result, we have:

$$\overline{F_c} = \overline{F_{cX}} = \frac{4\pi^2\kappa e}{(1-e^2)^{3/2}}\frac{GM_1M_2}{P_b^2w^2}\frac{M_2-M_1}{M_1+M_2}. \tag{17}$$

The force F_c acting on the system barycenter is directed from the pericentre of the heavy component orbit to the pericentre of the light component orbit. Precession of orbit pericentres makes the force F_c rotate in the direction of rotation of the components (i.e., counterclockwise in the selected reference frame). As a result, the binary system barycenter will move along a cycloidal trajectory with a periodically changing velocity. The equation of barycenter motion in the parametric form (we accept the rate of precession $\dot{\omega}$ is constant):

$$\begin{cases} x(t) = \dfrac{h}{\dot{\omega}^2}\left(1-\cos\left(\dot{\omega}t\right)\right), \\ y(t) = \dfrac{h}{\dot{\omega}^2}\left(\dot{\omega}t-\sin\left(\dot{\omega}t\right)\right), \end{cases} \tag{18}$$

where

$$h = \frac{4\pi^2\kappa e}{(1-e^2)^{3/2}}\frac{GM_1M_2}{P_b^2w^2}\frac{M_2-M_1}{(M_1+M_2)^2}.$$

Figure 1 shows the trajectories of some binary systems barycenters.

As can be seen, they are cycloids. Data on the height and step of these cycloids are given in table V.

Velocity v_c, maximum velocity $v_c^{\max}$ and average (time-based) velocity $\overline{v_c}$ of the barycenter motion are defined as follows:

$$v_c = \frac{\sqrt{2}h}{\dot{\omega}}\sqrt{1-\cos\left(\dot{\omega}t\right)};\ v_c^{\max} = \frac{2h}{\dot{\omega}};\ \overline{v_c} = \frac{4h}{\pi\dot{\omega}}. \tag{19}$$

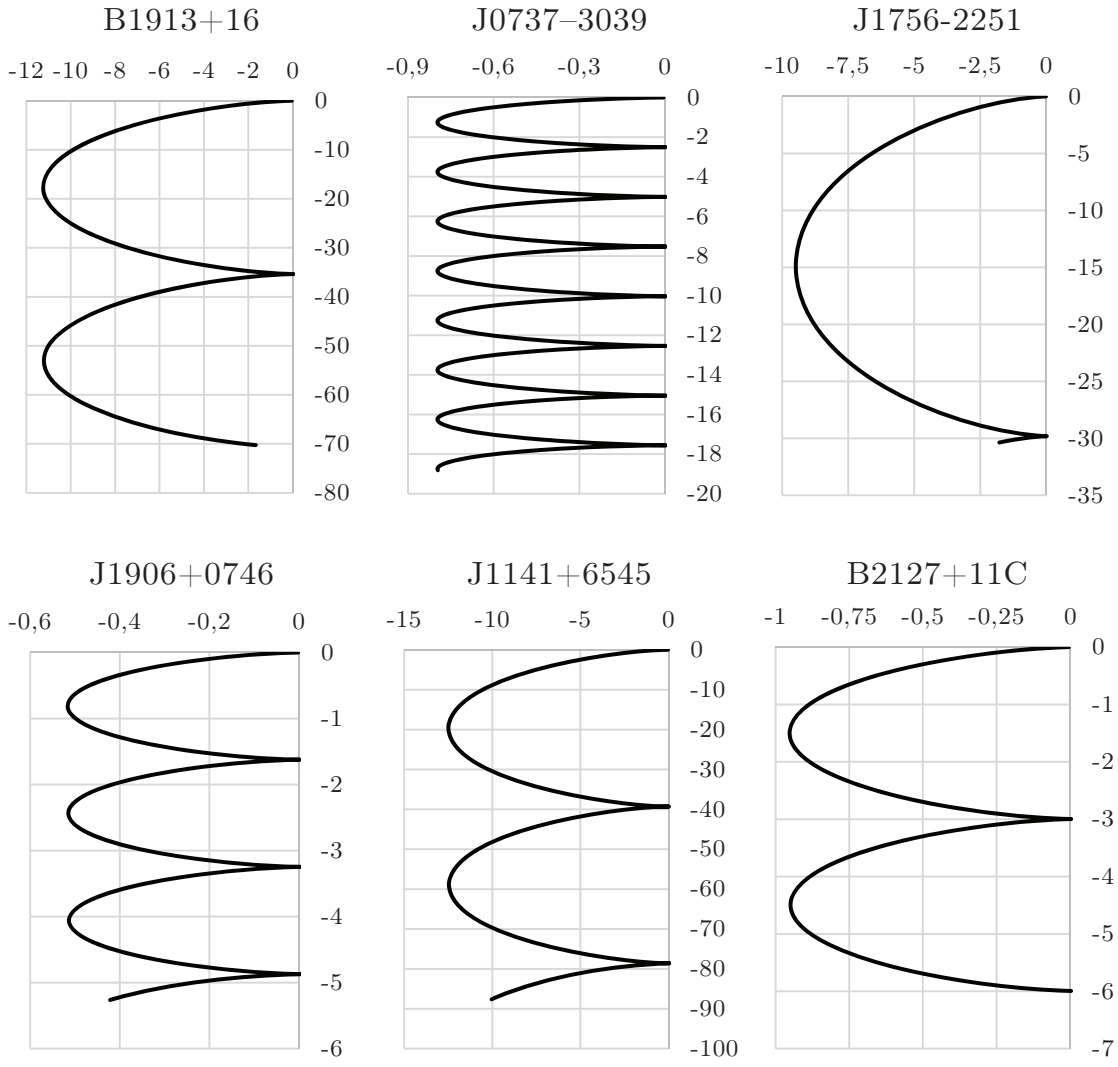

FIG. 1. Motion trajectories of binary systems barycenters for 160 years, $\times 10^{12}$ m

TABLE V. Parameters of cycloidal trajectories of binary systems barycenters, $\times 10^{12}$ m

PSR	height	base	PSR	height	base
B1913+16	11.24	35.36	J0737–3039	0.797	2.51
B2127+11C	0.952	3.00	J1756–2251	9.48	29.82
J1906+0746	0.516	1.62	J1141–6545	12.49	39.29

The detection of a periodic change in the barycenter velocity of the system will be an additional confirmation of the dependence of gravity on the velocity of the source and the "recipient" described in this article.

The smallest period of change in the velocity of motion of barycenter (from the number

of systems, for which there are reliable data on the masses of the components, table VI) has the system PSR J0737-3039. The period P_c of change in the velocity of the mass centre of this system is 21.3 years, maximum velocity — 1.854 km/s, average velocity — 1.18 km/s.

TABLE VI. Precession of some binary systems barycenters

PSR | Parameter	$P_c = 2\pi/\dot{\omega}$, years	$v_c^{\max}$, km/s	$\overline{v_c}$, km/s
B1913+16	85.2	6.553	4.172
J0737–3039	21.3	1.854	1.180
B2127+11C	80.6	0.323	0.206
J1756–2251	139.4	3.370	2.146
J1906+0746	47.5	0.539	0.343
J1141–6545	67.8	9.053	5.763

The accuracy of measuring the velocity of binary systems barycenters is currently low. According to [25], the velocity of the centre of mass of the PSR J0737–3039 system in the plane of the system is 96.0 ± 3.7 km/s. The error in determining this velocity, as we can see, is 2 times greater than the maximum velocity of the periodic motion of the barycenter.

The motion of binary systems barycenters can be revealed by observing the long-period oscillations of the heavy component radial velocity of the binary system (i.e., the observed velocity of approaching or moving away of the heavy component from the observer minus the constant component associated with the inertial motion of the system barycenter). The choice of the heavy component is because its velocity is lower; therefore, the amplitude of the relative velocity fluctuations is higher.

To determine the current velocity of the heavy component, we determine the values of the orbital velocity (v_{1x}, v_{1y}) projections on the x and y axes and the variable velocity of the barycenter (v_{cx}, v_{cy}).

Let us first determine the projection of the orbital velocity of the heavy component:

$$\begin{aligned} v_{1x} &= v\cos(u-\theta) = v(\cos u\cos\theta + \sin u\sin\theta) = v_0\sin\theta; \\ v_{1y} &= v\sin(u-\theta) = v(\sin u\cos\theta - \cos u\sin\theta) = v_0(\cos\theta - e), \end{aligned} \tag{20}$$

where θ is the angle between the radius vector of the heavy component and the x-axis; u is the angle between the radius vector of the heavy component and the orbital velocity:

$$\cos u = \frac{e\sin\theta}{\sqrt{1+e^2-2e\cos\theta}},\ \sin u = \frac{1-e\cos\theta}{\sqrt{1+e^2-2e\cos\theta}};$$

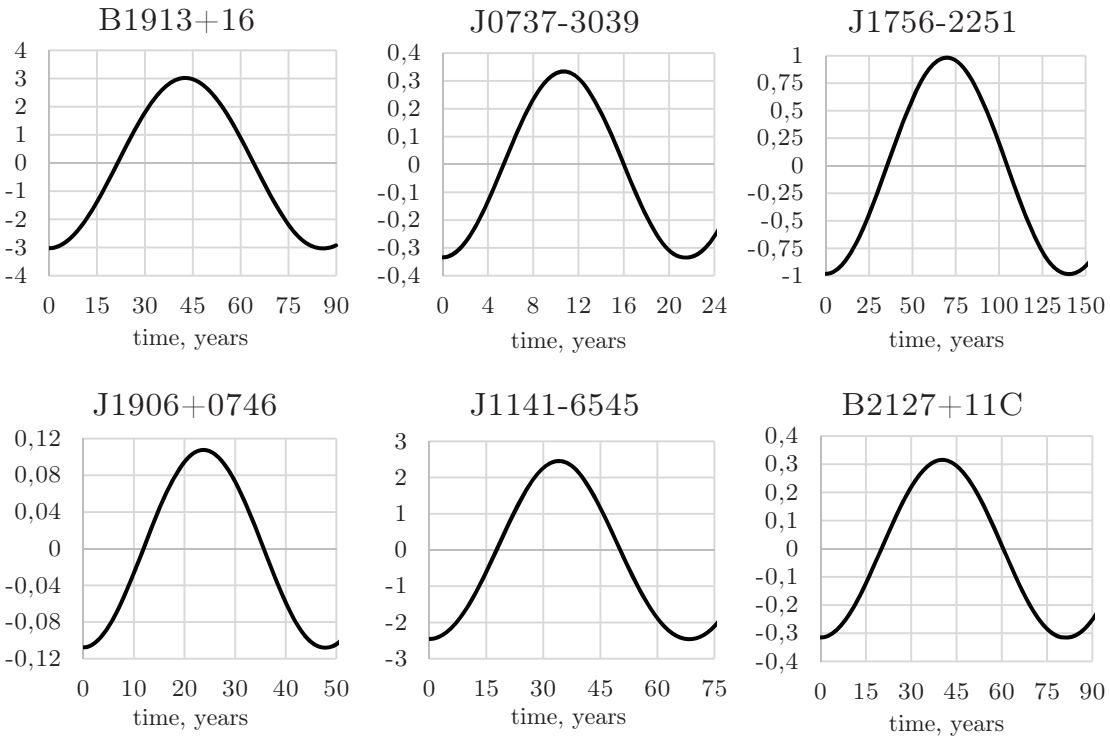

FIG. 2. Long-period oscillations of the minimum radial velocity of the heavy component,%

$$v_0 = \frac{1}{\sqrt{1-e^2}} \frac{M_2}{M_1+M_2} \sqrt{\frac{G\left(M_1+M_2\right)}{a}},$$

where M_2 is the mass of the light component.

Values of projections of the variable velocity of the barycenter:

$$v_{cx} = H\sin\varphi;\ v_{cy} = H\left(1-\cos\varphi\right), \tag{21}$$

where $H = h/\dot{\omega}$.

Total velocity of the heavy component of the binary system:

$$v = \sqrt{\left(v_0\sin\theta + H\sin\varphi\right)^2 + \left(v_0\left(\cos\theta - e\right) + H\left(1-\cos\varphi\right)\right)^2}. \tag{22}$$

We determine the values of the angle θ_0 at which (for a given value of φ) the velocity function v has extremes:

$$\frac{dv}{d\theta} = 0 \Rightarrow \theta_0 = -\arctan\left(\frac{H\sin\varphi}{H\cos\varphi - v_0 e - H}\right). \tag{23}$$

Let us now determine the values of the angle φ_0 at which (for $\theta = \theta_0$) the velocity function v has extremes:

$$\frac{dv}{d\varphi} = 0 \Rightarrow \varphi_0 = 0,\ \pi. \tag{24}$$

As a result we have:

$$v_{\max}(\varphi=\pi)=v_0(1-e)+2H;\ v_{\min}(\varphi=0)=v_0(1-e). \tag{25}$$

The relative amplitude of oscillations of the minimum values of heavy component's velocity (equal to the amplitude relative oscillations of its radial velocity):

$$\Delta v=\pm\frac{v_{\max}-v_{\min}}{v_{\max}+v_{\min}}=\pm\frac{H}{v_0(1-e)+H}. \tag{26}$$

Calculation by formula (26) gives the following values:

PSR	Δv, %	PSR	Δv, %	PSR	Δv, %
B1913+16	±3.03	B2127+11C	±0.31	J1906+0746	±0.11
J0737–3039	±0.33	J1756–2251	±0.98	J1141–6545	±2.45

Obtained values are confirmed by the simulation results (see Fig. 2).

IV. CONCLUSION

The coincidence of the precession values with the reality of the pericentres of the orbits, obtained as a result of numerical simulation, is a powerful argument in favour of the proposed dependence of gravity on the velocity of interacting bodies (see (9)). The indicated coincidence of the simulation results with reality is observed in all binary systems, in which other factors that affect the precession of the pericentre of the orbit (mass loss, tidal effects, etc.) do not appear substantially.

According to the dependence (9) confirmed in this article, with the gravitational interaction of bodies, in the general case, the force of gravitational action on the 2nd body from the 1st is not equal to the force of the gravitational action on the 1st body from the 2nd. Taking into account Newton's third law, the indicated difference of forces is possible only in the case when the gravitational interaction is carried out not directly between bodies, but through some intermediary, for example, a medium ("physical vacuum", "aether", etc.). In this case, the observance of Newton's third law is ensured in the interactions of the 1st body with the medium and the 2nd body with the medium.

For the final confirmation of the dependence of the gravitational interaction force on the velocity of motion-defined in this article, it is necessary to detect the motions of binary systems barycenters along the calculated cycloidal trajectories. Currently, there is no such

confirmation yet. As the results of measurements of the radial velocities of binary systems accumulate, the ability to detect the expected effect will steadily increase.

REFERENCES

[1] J. M. Weisberg et al. ASP Conf.Ser. 328, 25 (2005) arXiv:astro-ph/0407149v1

[2] M. Burgay et al. Nature 426, 531 (2003) arXiv:astro-ph/0312071v1

[3] I. H. Stairs et al. ApJ 581, 501 (2002) arXiv:astro-ph/0208357v1

[4] B. A. Jacoby et al. ApJ 644, L113 (2006) arXiv:astro-ph/0605375v1

[5] G. H. Janssen et al. A&A 490, 753–761 (2008) arXiv:astro-ph/0808.2292v1

[6] R. P. Mignani et al. Mon.Not.Roy.Astron.Soc. 430 (2), 1008 (2013) arXiv:astro-ph/1212.4801v1

[7] A.G. Lyne et al. Mon.Not.Roy.Astron.Soc. 312, 698 (2000) arXiv:astro-ph/9911313v1

[8] A. Corongiu et al. A&A 462, 703 (2007) arXiv:astro-ph/0611436v1

[9] J. G. Martinez et al. ApJ 812, 143 (2015) arXiv:astro-ph/1509.08805v1

[10] R. D. Ferdman et al. Mon.Not.Roy.Astron.Soc. 443 no.3, 2183 (2014) arXiv:astro-ph/1406.5507v1

[11] J. van Leeuwen et al. ApJ 798, 118 (2015) arXiv:astro-ph/1411.1518v1

[12] D. J. Champion et al.) Mon.Not.Roy.Astron.Soc. 350, L61 (2004) arXiv:astro-ph/0403553v1

[13] D. J. Champion et al. Mon.Not.Roy.Astron.Soc. 363, 929 (2005) arXiv:astro-ph/0508320v2

[14] J. K. Swiggum et al. ApJ 805, 156 (2015) arXiv:astro-ph/1503.06276v1

[15] J. P. W. Verbiest et al. The Twelfth Marcel Grossmann Meeting (Thibault Damour, Robert Jantzen and Remo Ruffini. Paris, World Scientific, 2012, 1571) arXiv:astro-ph/1210.0224v1

[16] M. Bailes et al. ApJ 595 L49 (2003) iopscience.iop.org/article/10.1086/378939/pdf

[17] M. B. Davies et al. Mon.Not.Roy.Astron.Soc. 335(2), 369 (2002) arXiv:astro-ph/0204511v1

[18] S. E. Thorsett et al. ApJ 405, L29 (1993) arXiv:astro-ph/9303002v2

[19] S. E. Thorsett et al. ApJ 512, 288 (1999) iopscience.iop.org/article/10.1086/306742/pdf

[20] E. M. Splaver et al. ApJ 581, 509 (2002) arXiv:astro-ph/0208281v1

[21] P. C. C. Freire et al. Mon.Not.Roy.Astron.Soc. 412, 2763 (2011) arXiv:astro-ph/1011.5809v1

[22] J. Khargharia et al. ApJ 744, 183 (2012) arXiv:astro-ph/1110.0507v1

[23] Kevin Brown. Reflections on Relativity (Lulu Enterprises Incorporated, 2016. p. 416)

[24] Paul Gerber. Zeitschrift für Mathematik und Physik. 43, 93 (1898)
archive.org/details/zeitschriftfrma14runggoog/page/n101/mode/2up

[25] S. M. Ransom et al. ApJ 609, L71-L74 (2004) arXiv:astro-ph/0404149v1